

Sulfated glycosaminoglycans and low-density lipoprotein receptor contribute to *Clostridium difficile* toxin A entry into cells

Liang Tao^{1,2,8,9}, Songhai Tian^{1,2,9}, Jie Zhang^{1,2,9}, Zhuoming Liu², Lindsey Robinson², Shin-Ichiro Miyashita^{1,2}, David T. Breault^{3,6,7}, Ralf Gerhard⁴, Siam Oottamasathien⁵, Sean Whelan², and Min Dong^{1,2}

¹Department of Urology, Boston Children's Hospital, and Department of Surgery, Harvard Medical School, Boston, MA 02115, USA

²Department of Microbiology and Immunobiology, Harvard Medical School, Boston, MA 02115, USA

³Division of Endocrinology, Boston Children's Hospital, Boston, MA 02115, USA

⁴Institute of Toxicology, Hannover Medical School, 30625 Hannover, Germany

⁵Department of Surgery and Pediatric Urology, University of Utah/Primary Children's Hospital, Salt Lake City, UT 84113, USA

⁶Department of Pediatrics, Harvard Medical School, Boston, MA 02115, USA

⁷Harvard Stem Cell Institute, Cambridge, MA 02138, USA

⁸Institute of Basic Medical Sciences, Westlake Institute for Advanced Study, Westlake University, Hangzhou, Zhejiang 310024, China

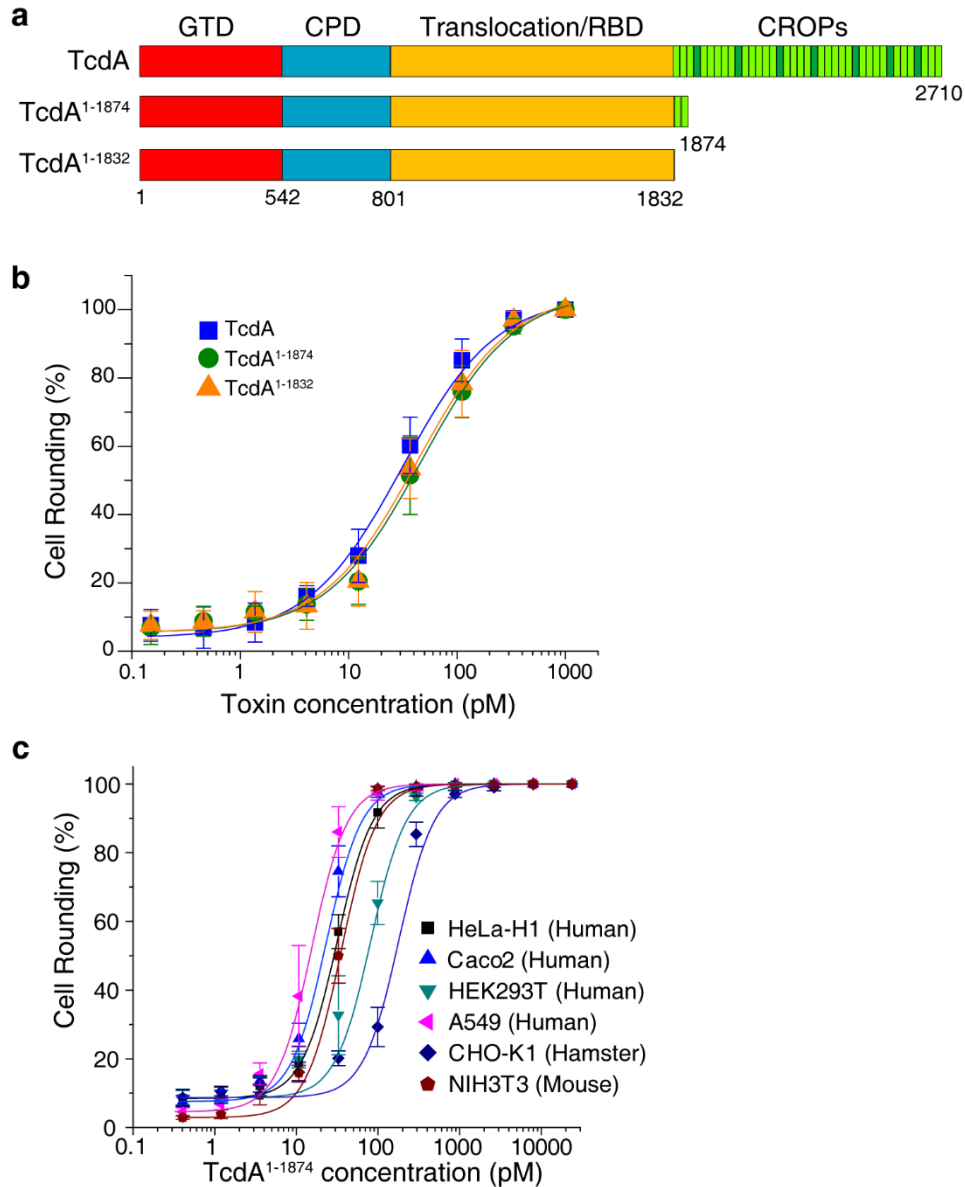
⁹These authors contributed equally to this work.

This file includes:

Supplementary Figures 1-9

Raw Image Figure

Supplementary Data Legend

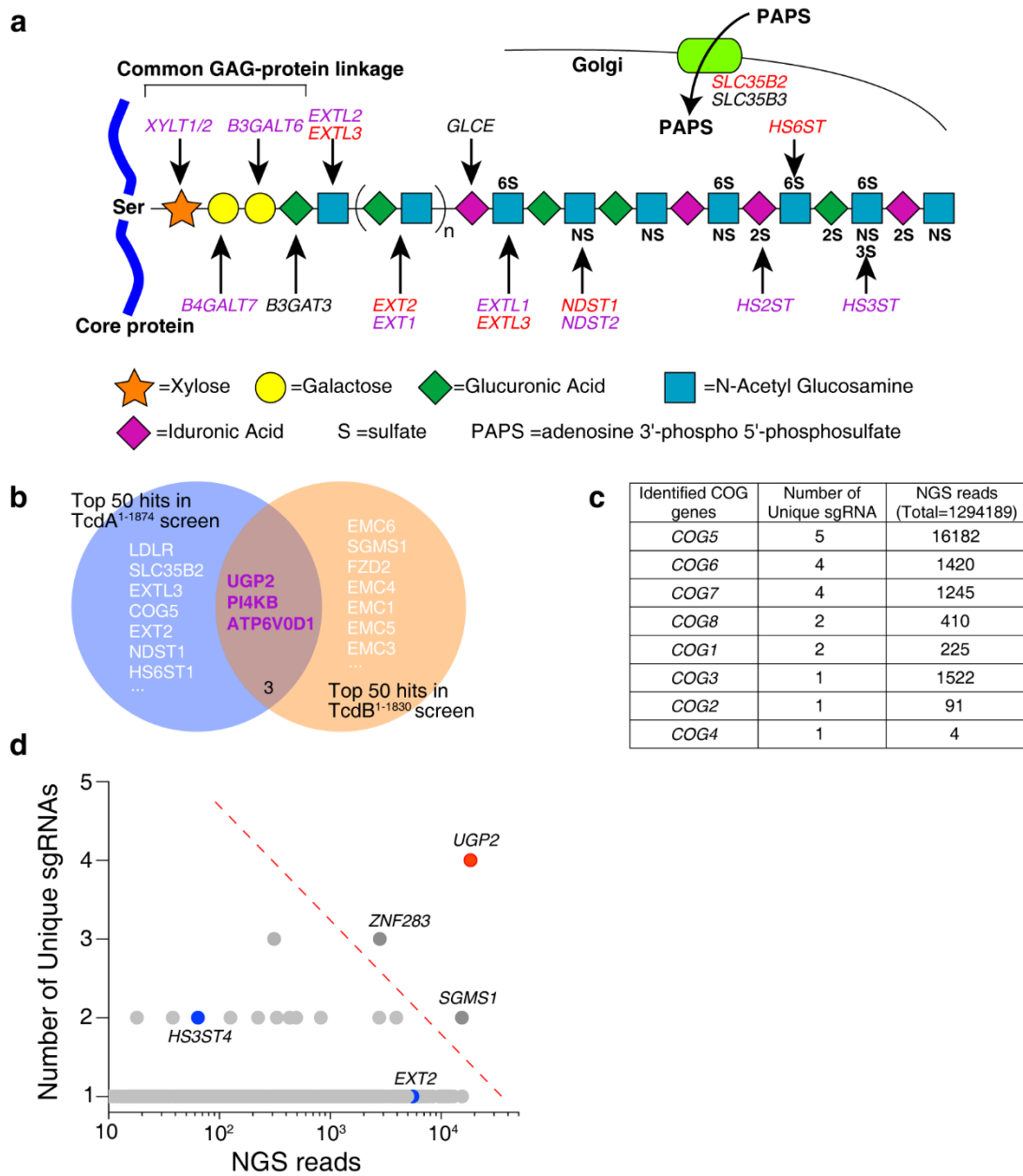


Supplementary Figure 1. Two truncated TcdA (TcdA¹⁻¹⁸³² and TcdA¹⁻¹⁸⁷⁴) lacking the CROPs retain potent toxicity on human cells.

a. Schematic drawing of TcdA, TcdA¹⁻¹⁸⁷⁴, and TcdA¹⁻¹⁸³². GTD: glucosyltransferase domain; CPD: cysteine protease domain; RBD: receptor binding domain; CROPs: combined repetitive oligopeptides.

b. The potency of the three TcdA variants on HeLa cells was determined using the cytopathic cell-rounding assays. The percentage of rounded cells were quantified, plotted, and fitted (data represent as mean \pm s.d., experiments were repeated in triplicates, n=4 (biological replicates)).

c. The sensitivities of HeLa, Caco-2, HEK293T, A549, CHO-K1, and NIH3T3 to TcdA¹⁻¹⁸⁷⁴ were estimated using the cytopathic cell-rounding assays. The percentage of rounded cells were quantified, plotted, and fitted (data represent as mean \pm s.d., experiments were repeated in duplicates, n=4 (biological replicates)).



Supplementary Figure 2. Schematic drawing of the HS synthesis pathways and analysis of top-ranked genes from CRISPR-Cas9 screens using TcdA¹⁻¹⁸⁷⁴ and full-length TcdA.

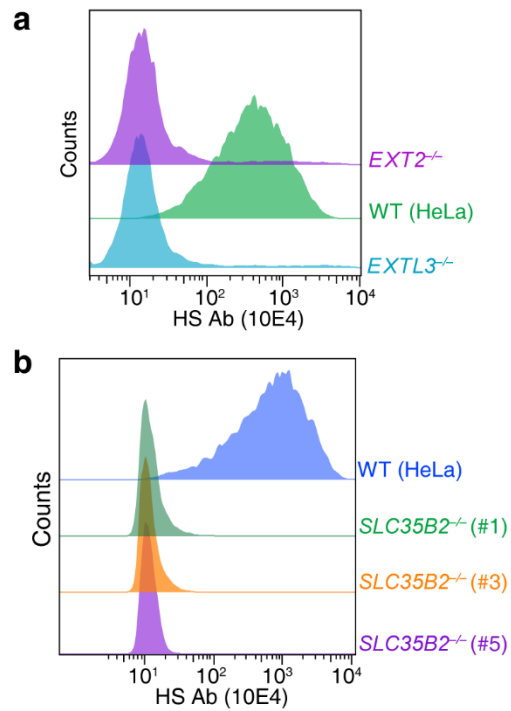
a. Schematic illustration shows genes involved in HS biosynthesis. Genes identified in R3 with more than 2 unique sgRNAs were marked in red, genes identified with 1 or 2 sgRNAs were marked in purple.

b. Comparison of top-50 ranked genes identified in genome-wide CRISPR-Cas9 screens for TcdA¹⁻¹⁸⁷⁴ versus in our previous screen with TcdB¹⁻¹⁸³⁰ (Ref.20). *UGP2*, *PI4KB*, and *ATP6V0D1* were the only three that overlapped between two screens.

c. All eight members of COG complex were identified in the TcdA¹⁻¹⁸⁷⁴ screen (R3).

d. Genome-wide CRISPR-Cas9-mediated screen was carried out on HeLa cells for full-length TcdA. Genes identified after TcdA screening were ranked and plotted. The y axis is the number of

unique sgRNA for each gene. The x axis represents the number of sgRNA reads for each gene. The top-ranking genes marked in red (*UGP2*) and dark gray (*ZNF283* and *SGMS1*). Two identified genes involved in HS biosynthesis are marked in blue.

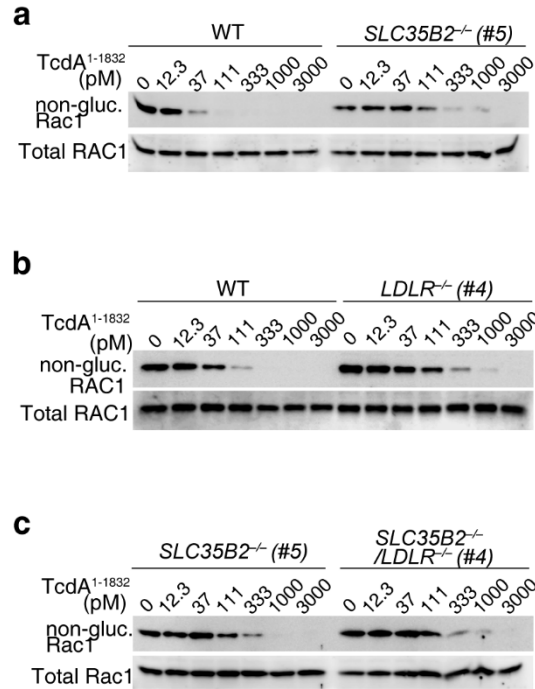


Supplementary Figure 3. Cells lacking *EXT2*, *EXTL3*, or *SLC35B2* lose surface HS expression.

a. The levels of cell surface HS in WT, $EXT2^{-/-}$, and $EXTL3^{-/-}$ HeLa cells were assessed by flow cytometry using a HS-specific antibody (10E4). $EXT2^{-/-}$ and $EXTL3^{-/-}$ cells showed greatly reduced levels of HS.

b. The cell surface HS in three $SLC35B2^{-/-}$ cell lines was assessed by flow cytometry using 10E4 antibody. All of the three cell lines showed greatly reduced levels of HS.

For panels **a** and **b**, experiments were repeated at least twice independently with similar results.



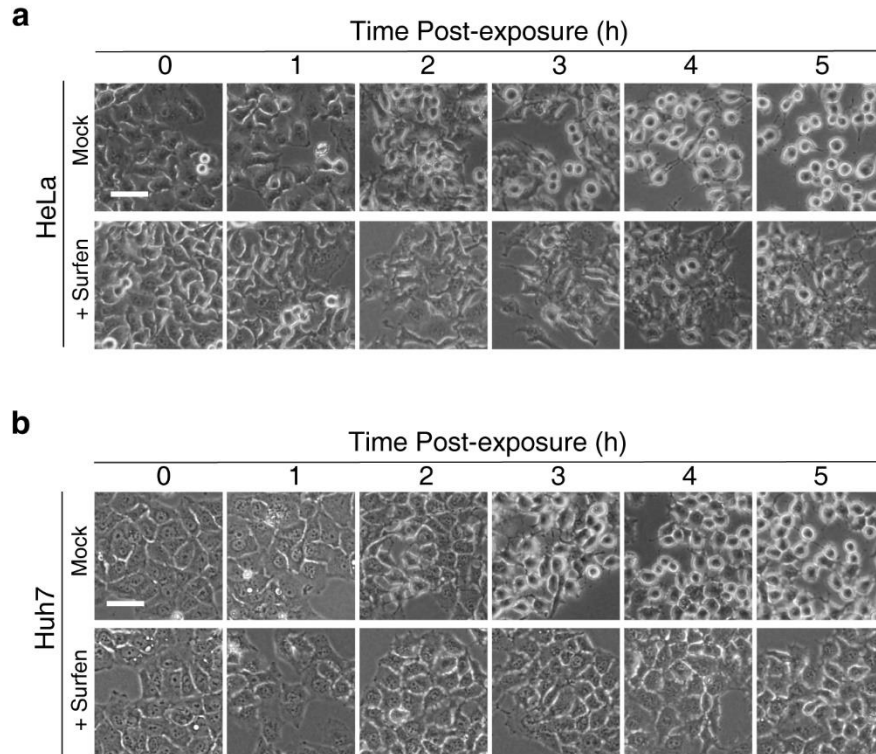
Supplementary Figure 4. RAC1 glucosylation in HeLa WT cells and the indicated KO cells after exposure to TcdA¹⁻¹⁸³².

a. The sensitivities of HeLa *SLC35B2*^{-/-} (#5) cells versus the WT cells to TcdA¹⁻¹⁸³² were compared by analyzing the glucosylation level of RAC1 via immunoblot assays.

b. The sensitivities of HeLa *LDLR*^{-/-} (#4) cells versus the WT cells to TcdA¹⁻¹⁸³² were compared by analyzing the glucosylation level of RAC1 via immunoblot assays.

c. The sensitivities of HeLa *SLC35B2*^{-/-} (#5) cells versus *LDLR*^{-/-}/*SLC35B2*^{-/-} (#4) cells to TcdA¹⁻¹⁸³² were evaluated based on the level of glucosylation of RAC1 protein.

For panels **a**, **b** and **c**, experiments were repeated at least twice independently with similar results.

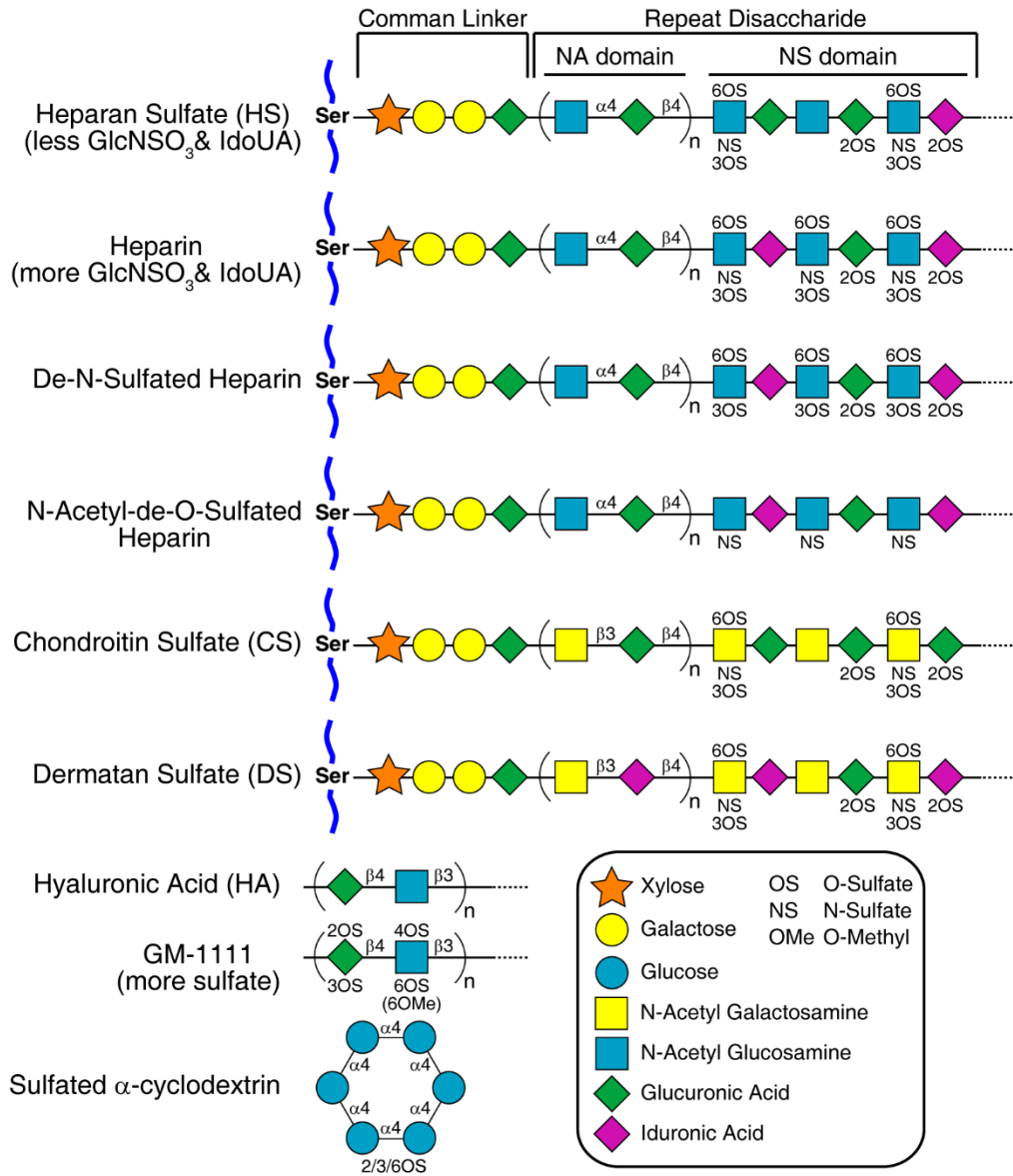


Supplementary Figure 5. Surfen protected cells from TcdA¹⁻¹⁸³².

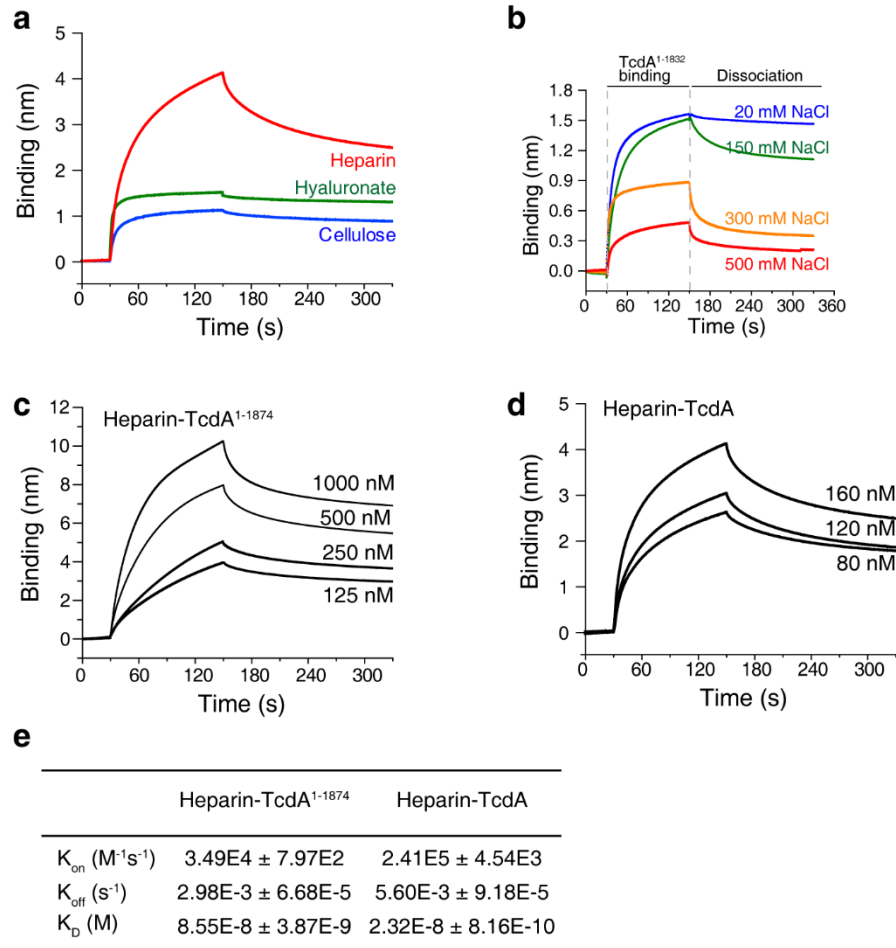
a. Representative images showing that pre-incubation of surfen (5 nM) reduced the cytopathic effect cause by TcdA¹⁻¹⁸³² (2 nM) in HeLa cells. Scale bar, 50 μ m.

b. Representative images showing that pre-incubation of surfen (5 nM) reduced the cytopathic effect cause by TcdA¹⁻¹⁸³² (2 nM) in Huh7 cells. Scale bar, 50 μ m.

For panels **a** and **b**, experiments were repeated at least three times independently with similar results.



Supplementary Figure 6. Schematic drawing of sGAGs and other sulfated molecules.



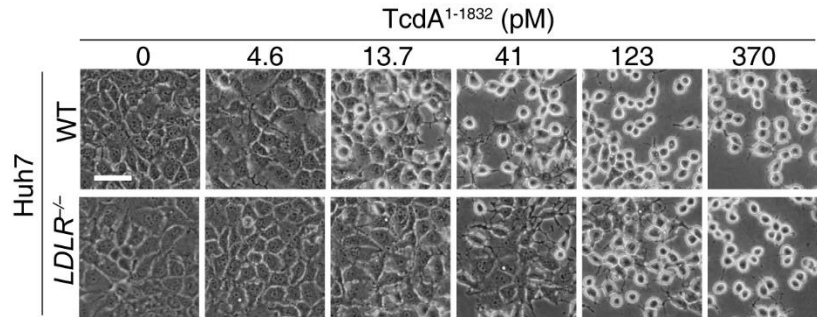
Supplementary Figure 7. Characterizing binding of TcdA¹⁻¹⁸⁷⁴ to heparin using BLI assay.

a. Direct binding of full-length TcdA to immobilized biotin-heparin was analyzed using BLI assays. Biotin-hyaluronate and biotin-cellulose were analyzed in parallel as controls.

b. Direct binding of TcdA¹⁻¹⁸⁷⁴ to immobilized heparin was sensitive to salt concentrations.

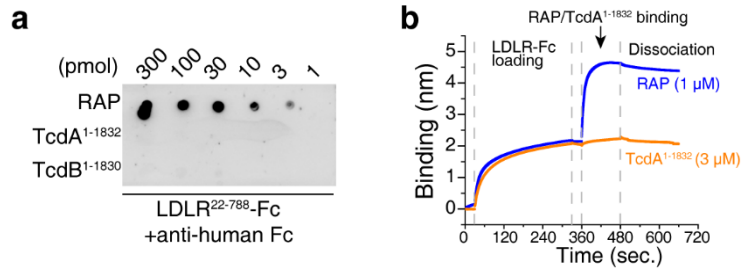
c-e. The binding affinity between heparin and TcdA¹⁻¹⁸⁷⁴ (panel c) or between heparin and full-length TcdA (panel d) in TBS buffer (20 mM Tris-Cl, 150 mM NaCl, pH 7.5) was measured by BLI assay. The binding kinetic data were listed in panel e (n=3, Centre values represent mean. Error bars represent \pm s.d.).

Representative data was shown from two independent experiments.



Supplementary Figure 8. Representative images showing that Huh7 *LDLR*^{-/-} cells are less sensitive to TcdA¹⁻¹⁸³² than WT cells.

Huh7 *LDLR*^{-/-} cells were less sensitive to TcdA¹⁻¹⁸³² compared with the WT cells using the cytopathic cell-rounding assays (12 h incubation). Scale bar, 50 μ m. The experiments were repeated at least three times independently with similar results.



Supplementary Figure 9. Binding of LDLR-Fc to TcdA¹⁻¹⁸⁷⁴ was not detected.

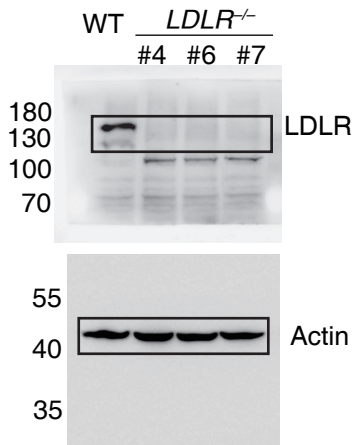
a. *In vitro* dot blot assays did not detect binding of LDLR-Fc to immobilized TcdA¹⁻¹⁸⁷⁴. RAP and TcdB¹⁻¹⁸³⁰ served as positive and negative control respectively.

b. BLI analysis showed that 1 μM RAP robustly bound to immobilized LDLR-Fc, while TcdA¹⁻¹⁸⁷⁴ at up to 3 μM had no detectable binding.

The experiments were repeated at least three times independently with similar results.

Raw Image Figures

Figure 3a



Supplementary Figure 4a

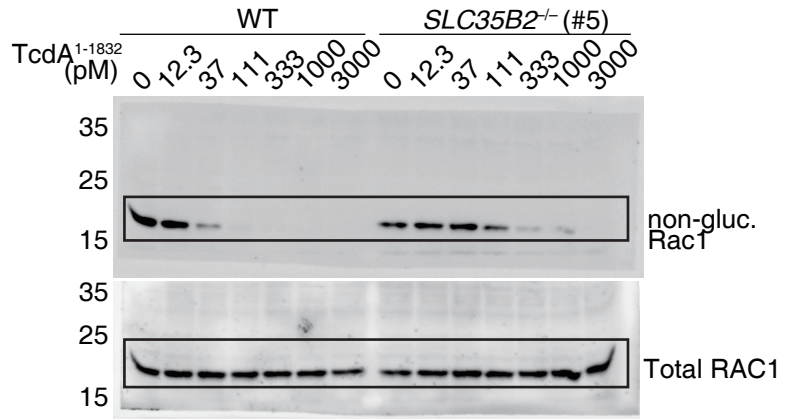
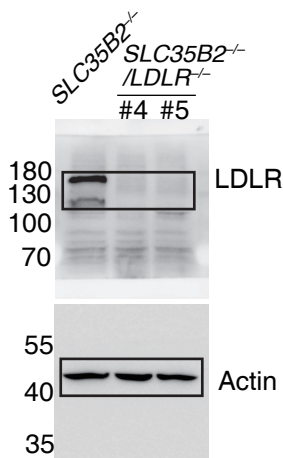
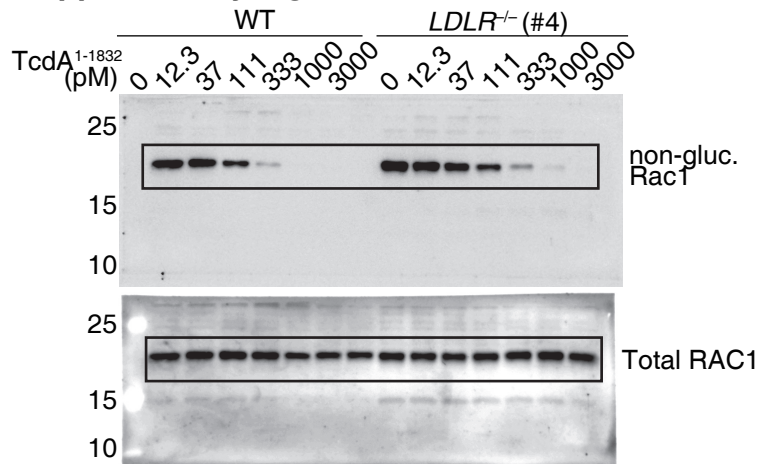


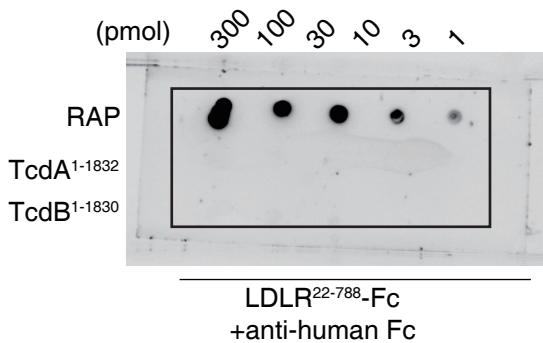
Figure 4a



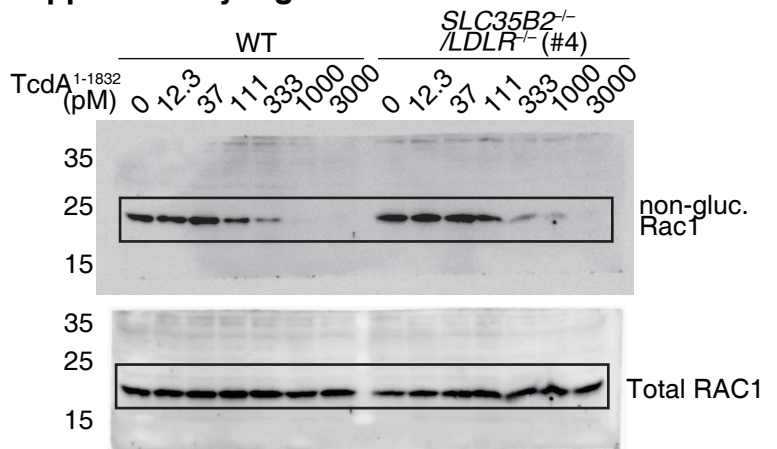
Supplementary Figure 4b



Supplementary Figure 9a



Supplementary Figure 4c



Supplementary Data (for Figure 1) | Lists of all sgRNA sequences and target genes identified from CRISPR-Cas9 screen.

Column A: Gene name; Column B: sgRNA code name; Column C: sgRNA sequence; Column D: NGS reads.

Sheet 1: Library A screened with TcdA¹⁻¹⁸⁷⁴.

Sheet 2: Library B screened with TcdA¹⁻¹⁸⁷⁴.